ACS OMEGA

Open Access

http://pubs.acs.org/journal/acsodf

Article

Nanoencapsulated Curcumin Mitigates Liver Injury and Drug-Metabolizing Enzymes Induction in Diclofenac-Treated Mice

Suhair Sunoqrot,* Mohammad Abu Shalhoob, Yazun Jarrar, Alaa M. Hammad, Hamzeh J. Al-Ameer, and Wajdy Al-Awaida

Cite This: *ACS Omega* 2024, 9, 7881−7890

Read Online

ACCESS | Metrics & More | Article Recommendations

ABSTRACT: Curcumin (CUR) is a natural product with known anti-inflammatory, antioxidant, and hepatoprotective properties. The aim of this study was to formulate CUR into a polymeric nanoparticle (NP) formulation and examine its potential hepatoprotective activity in an animal model of diclofenac (DIC)-induced hepatotoxicity. CUR was loaded into polymeric NPs composed of poly(ethylene glycol)-polycaprolactone (PEG−PCL). The optimal CUR NPs were evaluated against DIC-induced hepatotoxicity in mice, by studying the histopathological changes and gene expression of drug-metabolizing *cyp450* (*cyp2c29* and *cyp2d9*) and *ugt* (*ugt2b1*) genes in the livers of the animals. The optimal NPs were around 67 nm in diameter with more than 80% loading efficiency and sustained release. Histological findings of mice livers revealed that CUR NPs exhibited a superior hepatoprotective effect compared to free CUR, and both groups reduced DIC-mediated liver tissue injury. While treatment with DIC alone or with CUR and CUR NPs had no effect on *cyp2c29* gene expression, *cyp2d9* and *ugt2b1* genes were upregulated in the DIC-treated group, and this effect was reversed by CUR both as a free drug and as CUR NPs. Our findings present a promising application for nanoencapsulated CUR in the treatment of nonsteroidal anti-inflammatory drugs-induced liver injury and the associated dysregulation in the expression of hepatic drug-metabolizing enzymes.

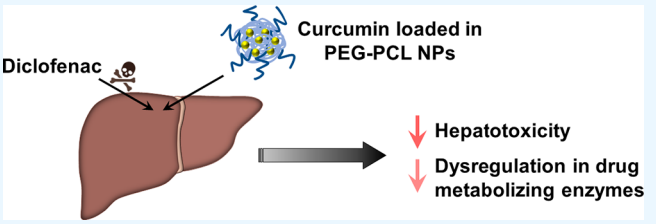

INTRODUCTION

The liver is the main organ responsible for detoxification of drugs and xenobiotics.[1] This function is enabled by the actions of Phase I and Phase II metabolizing enzymes that ultimately aim to increase the hydrophilicity of drugs and facilitate their elimination from the body.[2] Cytochrome P450 (CYP) enzymes are the most well-known drug-metabolizing enzymes that carry out Phase 1 metabolism, whereas uridine 5′-diphosphate (UDP) glucuronosyltransferases (UGTs) are examples of Phase II metabolizing enzymes.[1,3] Drug-related hepatotoxicity is considered one of the main causes of acute liver failure in the United States and Europe.[4,5] Many drugs are metabolically inactivated by CYP enzymes to produce electrophilic reactive metabolites which then create a CYP-metabolite combination by covalently connecting with the same CYP.[6] Reactive metabolites can also cause cell stress by reacting with biological components, such as proteins, DNA, and membranes. The development of reactive metabolites may end in toxic hepatitis, which can occur following overdoses, or immuno-allergic hepatitis, occurring when the drug stimulates an unfavorable immunological reaction against the liver.[2,7]

Nonsteroidal anti-inflammatory drugs (NSAIDs) are one of the most widely prescribed drug classes. NSAIDs are mainly metabolized by the liver and are associated with a range of side effects mainly affecting the gastrointestinal, renal, and cardiovascular systems.[8−10] Most patients taking therapeutic doses of NSAIDs can tolerate them well. However, a higher risk of NSAID-induced toxicity may occur upon chronic use and in the presence of comorbidities.[11] Diclofenac (DIC) is the most widely used NSAID worldwide among the various NSAIDs.[12] Like other NSAIDs, DIC is associated with dose-related gastrointestinal, cardiovascular, and renal adverse effects.[13] DIC is also associated with a high risk of drug-induced liver injury.[14] After oral administration, DIC is rapidly absorbed from the human intestine and is detoxified via hydroxylation and glucuronidation. Hydroxylation occurs by the action of CYP2C9 and 3A4 to form 4′-hydroxy and 5-hydroxy derivatives, whereas glucuronidation occurs via UGT isozymes UGT1A9 and 2B7.[15] In addition to its hepatotoxicity, DIC causes an increase in apoptosis through changes in hepatic mitochondrial activity and the formation of reactive

Received: October 4, 2023
Revised: January 5, 2024
Accepted: January 19, 2024
Published: January 31, 2024

Scheme 1. Synthesis of PEG−PCL Copolymer

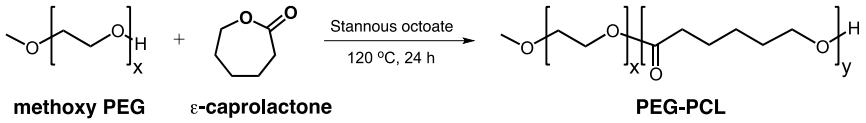

oxygen species (ROS), and this change is most probably due to CYP-mediated metabolism.[16]

In a recent study, the administration of the NSAIDs mefenamic acid, ibuprofen, and meloxicam, but not DIC, downregulated the expression of arachidonic acid (AA)-metabolizing *cyp450* genes in the livers of experimental mice after 14 days of treatment, which was accompanied by histological alterations indicative of liver injury.[17] Furthermore, NSAIDs including DIC downregulated *ugt2b1* gene expression in the liver, kidney, and heart of experimental mice after 14 days of treatment.[18] Another study found that DIC and its metabolites can directly induce acute hepatotoxicity, with DIC-glucuronide implicated in inducing acute immune activation and cell death in the liver.[14]

Since increased oxidative stress is among the key mediators of drug-induced liver injury, various natural antioxidants have been investigated as hepatoprotective agents.[19,20] Among these bioactive compounds, curcumin (CUR) has received a lot of attention for its potent antioxidant, anticancer, antimicrobial, anti-inflammatory, and cardioprotective properties.[21−23] According to in vitro and in vivo investigations, CUR may protect hepatocytes by decreasing the formation of reactive species and tissue necrosis factor alpha (TNF-α) in lipopolysaccharide (LPS)-induced hepatotoxicity.[24] Curcuminoids and piperine supplementation had a hepatoprotective effect in patients with nonalcoholic fatty liver disease.[25] A CUR-galactomannoside complex demonstrated hepatoprotective effects in chronic alcoholics by lowering transaminases and gamma-glutamyl transferase levels, as well as increasing endogenous antioxidants and decreasing inflammatory markers.[26] However, CUR has pharmaceutical disadvantages in terms of limited water solubility, poor oral bioavailability, and low in vivo stability, which has been a motivation for developing various delivery systems, particularly those based on nanotechnology.[27−29] Different types of drug delivery nanocarriers or nanoparticles (NPs) can be readily fabricated from organic or inorganic materials.[30,31] Among those, polymeric NPs have proven their efficiency in the encapsulation of many synthetic and natural drugs and have shown successful delivery in vitro and in vivo.[32]

The aim of this study was to investigate the role of CUR, in its free and NP forms, in DIC-induced liver injury and the status of hepatic metabolic enzymes. To achieve this aim, CUR was encapsulated in biodegradable polymeric NPs composed of poly(ethylene glycol)-*b*-poly(ε-caprolactone) (PEG−PCL). Then, CUR and CUR NPs were tested as potential hepatoprotective agents against DIC-induced hepatotoxicity in a mouse model by studying the histopathological changes and gene expression of drug-metabolizing *cyp* (*cyp2c29* and *cyp2d9*) and *ugt* (*ugt2b1*) genes in the livers of the experimental mice.

MATERIALS AND METHODS

Materials. CUR, tin(II) 2-ethylhexanoate (stannous octoate), ε-caprolactone (CL), and methoxy PEG (MW 5,000) were obtained from Sigma-Aldrich (St. Louis, MO, USA). Dimethyl sulfoxide (DMSO) and dichloromethane (DCM) were purchased from Fisher Chemical (Loughbough, UK). Diethyl ether and dimethylformamide (DMF) were procured from Tedia (Fairfield, OH, USA). Water used throughout the study was of ultrapure grade (Millipore Direct-Q 5UV, Millipore, Billerica, MA, USA). DIC (as DIC deanolate; Tratul) was obtained from Gerot lannach (Vienna, Austria). The TRIzol solution and cDNA synthesis kit were acquired from Thermo Fisher Scientific (Massachusetts, USA). SYBR Green Master Mix was obtained from Bio-Rad (Hercules, CA, USA). Primers were purchased from Integrated DNA Technologies (Coralville, Iowa, USA).

Synthesis of PEG−PCL Copolymer. PEG−PCL copolymer was synthesized by ring-opening polymerization of CL in the presence of methoxy PEG as a macroinitiator and stannous octoate as a catalyst as reported in an earlier publication (Scheme 1).[33] For the synthesis, 1 g of PEG and 2 g of CL were weighed in a 100 mL round-bottom flask and dried under vacuum for 2 h. Stannous octoate (3 drops; ca. 30 mg) was injected into the flask using a glass syringe (Caution: avoid contact with skin and eyes and avoid inhalation). The flask was then heated in an oil bath to 120 °C, and the reaction was carried out under moderate stirring (120 rpm) for 24 h. The crude product was cooled to room temperature, dissolved in DCM, and precipitated in cold diethyl ether. All procedures were carried out under a chemical fume hood and standard personal protective equipment were used. Finally, the product was vacuum filtered and stored in a desiccator at room temperature.

Spectroscopic Characterization of PEG−PCL. The chemical structure of the synthesized copolymer was confirmed by Fourier transform infrared (FTIR) and nuclear magnetic resonance (NMR) spectroscopy. For FTIR analysis, a powder sample of PEG−PCL was prepared as a KBr disk, and the spectrum was acquired by using an IR Affinity-1 spectrometer (Shimadzu, Kyoto, Japan). For ^{1}H NMR analysis, approximately 20 mg of the copolymer was dissolved in $CDCl_3$, and the spectrum was obtained using a Bruker 500 MHz Avance III instrument (USA).

Preparation of CUR NPs. CUR was loaded into PEG−PCL NPs by nanoprecipitation.[34] The organic phase was prepared by mixing 1, 2, or 4 mg of CUR (from a 20 mg/mL stock solution in DMF) with 20 mg of PEG−PCL and completing the volume up to 1 mL with DMF. The organic solution was then added dropwise to 10 mL of ultrapure water in a glass vial under stirring for 1 h to obtain a colloidal dispersion. The NPs were purified by dialysis against 2 L of deionized water (12−14 kDa molecular weight cut-off (MWCO) membrane, Spectrum Laboratories Inc., Repligen, USA). The dialysis was maintained for 24 h, with the water changed every 6 h, after which the NPs were collected for further characterization.

Characterization of CUR NPs. *Dynamic Light Scattering (DLS).* Dynamic light scattering (DLS) was employed to measure the particle size and polydispersity of the NPs using a Nicomp Nano Z3000 instrument (Entegris, Billerica, MA, USA). Fresh samples were diluted with ultrapure water (1:1)

https://doi.org/10.1021/acsomega.3c07602
ACS Omega 2024, 9, 7881−7890

for the measurement. The results were reported as the mean ± standard deviation (SD) of three different NP batches.

Loading Efficiency Determination. Fresh NPs were diluted 100× in DMSO to release loaded CUR. Drug loading was measured by UV−vis spectroscopy (Shimadzu UV-1800 spectrophotometer, Kyoto, Japan) based on a calibration curve of CUR in DMSO at λ_{max} = 430 nm. Loading efficiency was calculated according to the following equation:

$$\text{Loading efficiency (\%)} = \frac{\text{Actual weight of loaded CUR}}{\text{Theoretical weight of loaded CUR}} \times 100\%$$

In Vitro Release of CUR from CUR NPs. CUR release was investigated in phosphate-buffered saline (PBS; pH 7.4) containing 0.5% w/v Tween 80 to ensure sink condition. One milliliter of fresh CUR NPs was placed in a 3.5 kDa MWCO dialysis membrane in triplicate. Another set of triplicate samples contained 1 mL of free CUR (1 mg/mL in DMSO). Each sample was immersed in 30 mL of the release buffer and placed in an orbital shaking incubator (Biosan ES-20, Riga, Latvia) at 37 °C and 100 rpm. At defined time points, 10 mL samples were withdrawn from the release medium and replaced with an equivalent volume of fresh medium. The fluorescence of the samples was recorded using a Synergy HTX Multi-Mode Reader (BioTek, Winooski, VT, USA) at 460/40 nm excitation and 528/20 nm emission wavelengths. CUR NPs and free CUR remaining in the dialysis bags at the end of the release experiment were diluted 10× with DMSO, and their fluorescence was recorded to obtain the amount of CUR remaining in each sample. The amount of CUR released or remaining in the bags was calculated based on a calibration curve of CUR fluorescence versus concentration in the release medium or DMSO. The cumulative percent amount of CUR released versus time was plotted to form the release profile.

DIC-Induced Liver Injury Animal Model. *Animals.* Thirty-five male Balb/c mice weighing between 27 and 38 g and aged 8 weeks were obtained from the Applied Science Private University (Amman, Jordan). The Canadian Council on Animal Care guidelines were followed for animal handling,[35] and the study protocol was approved by Al-Zaytoonah University of Jordan's Animal Care and Use Committee. All mice were housed and kept at a temperature of 23 ± 1 °C with a 12 h light/12 h dark cycle and kept on standard laboratory animal diet pellets ad libitum.

Experimental Protocol. The mice were divided into five groups, with each group containing seven mice. Mice were randomly assigned according to Table 1.

Table 1. Animal Groups and Treatments

group	treatment[a]
control	normal saline + PEG 400[b] (negative control)
DIC	10 mg/kg DIC (positive control)
DIC+CUR	10 mg/kg DIC + 20 mg/kg CUR
DIC+CUR NPs	10 mg/kg DIC + CUR NPs[c]
DIC+PEG−PCL NPs	10 mg/kg DIC + PEG−PCL NPs[d]

[a]All treatments were administered as a single intraperitoneal (IP) injection once a day. [b]DIC and CUR vehicle [c]Equivalent to 20 mg/kg CUR and dispersed in ultrapure water. [d]Equivalent to CUR NPs and dispersed in ultrapure water.

DIC toxicity begins to appear clearly from the 14th day of treatment or more.[17,36] Therefore, treatments with DIC were carried out for 23 days. DIC+CUR and DIC+CUR NPs groups were first given CUR and CUR NPs (20 mg/kg equivalent to CUR) without DIC as pretreatment for two consecutive days; then on the third day, both groups were given CUR and CUR NPs with DIC for 23 additional days. DIC+CUR, DIC+CUR NPs, and DIC+PEG−PCL NPs groups received their daily injections of CUR, CUR NPs, or PEG−PCL NPs, respectively, 3 h before being administered their daily DIC injections. Mice weights were measured five times during the study. The weight measurements were taken on the first, seventh, 14th, 21st, and 25th (last) days of drug administration (including 2 days of pretreatment with CUR and CUR NPs followed by 23 days of DIC treatment). At the end of the study, animals were sacrificed using diethyl ether and cervical dislocation, and then the livers were excised for further analysis.

Histological Analysis. After the mice were euthanized, the livers were removed and fixed in 10% formalin. The samples were dehydrated by placing them through a graded series of alcohol (70, 80, 90, 95, and 100%) followed by xylene as a clearing agent. The liver tissues were then immersed in a molten paraffin wax. The liver slides were stained with hematoxylin and eosin. Finally, the prepared slides were imaged using a Leica microscope equipped with a digital camera.

RNA Extraction and cDNA Synthesis. After the mice were sacrificed, around 200 mg of liver tissue was taken from each one. The liver tissue samples were homogenized using a Direct-zol RNA MiniPrep Kit (Zymo-Research, USA; catalog no. R2052), and the mRNA was isolated following the manufacturer's instructions. The mRNA concentration in each sample was analyzed using a Nanodrop DNA/Protein Analyzer (Quawell, Sunnyvale, CA, USA). The extracted mRNA was then converted to cDNA using a cDNA synthesis kit (Thermo Fisher Scientific) following the manufacturer's instructions. The purity of the cDNA samples was determined by adding 1 μL of each sample to a Nanodrop analyzer (Quawell) and estimating the ratio of absorbance at 260 nm/280 nm. The RNA/cDNA ratios were about 2 ± 0.1 and 1.8 ± 0.1, respectively, indicating that the samples were within acceptable purity ratios.

Gene Expression Analysis. This study investigated the relative mRNA expression of the *cyp2c29*, *cyp2d9*, and *ugt2b1* genes, which are equivalent to the human genes *CYP2C9, CYP2D6,* and *UGT2B7,* respectively. Table 2 shows the sequence of primers and the applicant sizes for each amplified gene. The expression levels of the target genes were investigated using quantitative real-time polymerase chain reaction (RT-PCR) as previously described.[37] In summary, up to 100 ng of synthesized cDNA were mixed with 10 pmol of forward and reverse primers in a reaction mixture including SYBR Green master mix. The following were the PCR conditions: denaturation at 95 °C for 30 s, then 40 cycles of denaturation at 95 °C for 10 s, and annealing at 55 °C for 30 s. In this investigation, the *gapdh* gene was employed as a housekeeping gene, and the expression of the genes was determined using the ΔΔCT method.[38]

Statistical Analysis. The change in relative mRNA expression of the gene of interest following different treatment conditions was expressed as a fold change relative to the control. One-way analysis of variance (ANOVA) was used to compare the control and other groups, followed by Tukey's

https://doi.org/10.1021/acsomega.3c07602
ACS Omega 2024, 9, 7881−7890

Table 2. Primer Sequences and Applicant Sizes of *cyp2c29*, *cyp2d9*, *ugt2b1*, and *gapdh* Genes

gene name	forward	reverse	size	reference
cyp2c29	AGGAGTTTCCCAACCCAGAG	TTCTTTTGGGTGGACCAGAG	203	17
cyp2d9	AAGGCTGGCTGACAAGGCCC	TCGGGGTGCTTGGACAGGGT	219	17
ugt2b1	GGGAGCAGCTGTTAGAGTGG	TTGCGCATGACATACTCGAT	183	18
gapdh	CCCCAATGTATCCGTTGTG	TAGCCCAGGATGCCCTTTAGT	124	39

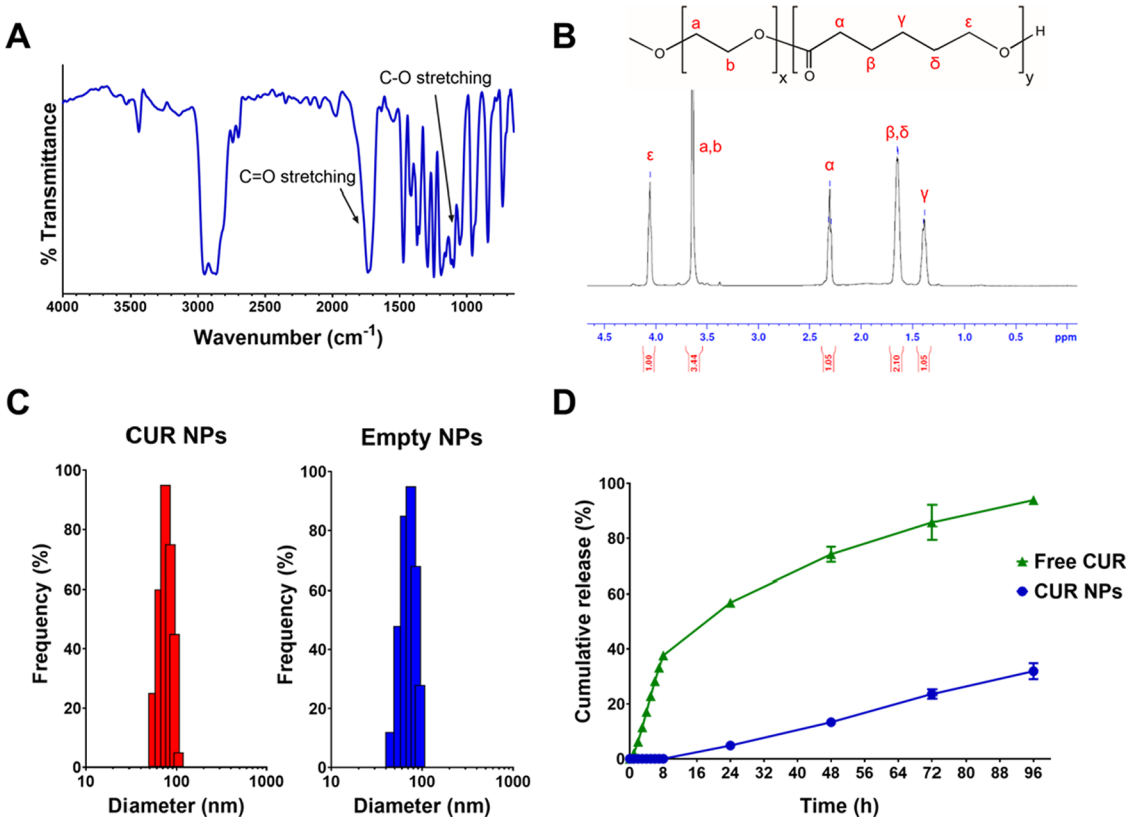

Figure 1. (A) FTIR and (B) ^{1}H NMR spectra of PEG−PCL copolymer; (C) representative particle size distributions of CUR NPs (F3) and empty NPs; (D) in vitro release profile of CUR from F3 compared to free CUR at pH 7.4 up to 96 h (mean ± SD, n = 3).

post-hoc analysis using GraphPad Prism 7 software. When the p-value was less than 0.05, the change in the mRNA expression of the tested genes was considered statistically significant.

RESULTS

Preparation and Characterization of CUR-Loaded PEG−PCL NPs. PEG−PCL was employed in this study to encapsulate CUR as it has previously shown promising results in loading plant polyphenols.[33,40] PEG−PCL was synthesized by ring-opening polymerization and characterized by FTIR and ^{1}H NMR. In the FTIR spectrum (Figure 1A), the polymer exhibited a C−H stretching band at 2970 cm^{-1}, a sharp C═O stretching band at 1730 cm^{-1} referring to the ester carbonyl groups of PCL, and a C−O stretching band between 1100 and 1500 cm^{-1} corresponding to the ether groups of PEG. ^{1}H NMR was utilized to further verify the copolymer's structure and estimate the MW of the PCL block (Figure 1B).[33] Based on the relative integration ratio of the proton peaks referring to the ethylene oxide units (a and b) and the proton peaks of the CL chain (ε), the PCL block's MW was estimated to be 7450 Da. The synthesized PEG−PCL copolymer was then used to prepare CUR NPs by nanoprecipitation. The CUR:polymer ratio was varied to maximize drug loading. As presented in Table 3, CUR was successfully entrapped in PEG−PCL NPs with particle sizes ranging from 64 to 67 nm and with a loading efficiency range from 82.4 to 93.1%. The NPs also had a narrow size distribution, as indicated by their low polydispersity index (PDI) values ranging from 0.08 to 0.09. The empty PEG−PCL NPs (without CUR) showed a hydrodynamic diameter similar to that of CUR NPs (Figure 1C). Having shown the best loading efficiency, F3 containing 4 mg CUR/20 mg PEG−PCL was chosen for subsequent investigations.

Table 3. Characteristics of CUR NPs (Mean ± SD; n = 3)

sample	CUR (mg)	PEG−PCL (mg)	particle size (nm)	PDI	loading efficiency (%)
F1	1	20	66.4 ± 8.4	0.09 ± 0.02	82.4 ± 4.6
F2	2	20	64.0 ± 4.6	0.08 ± 0.00	90.0 ± 12.8
F3	4	20	67.4 ± 7.0	0.09 ± 0.01	93.1 ± 3.9

In Vitro Release of CUR from CUR NPs. CUR release from the optimized PEG−PCL NP formulation (F3) was monitored for 96 h under physiological conditions (pH 7.4, 37 °C). As shown in Figure 1D, CUR NPs showed zero % release during the first 8 h, followed by slow release up to 96 h.

https://doi.org/10.1021/acsomega.3c07602
ACS Omega 2024, 9, 7881−7890

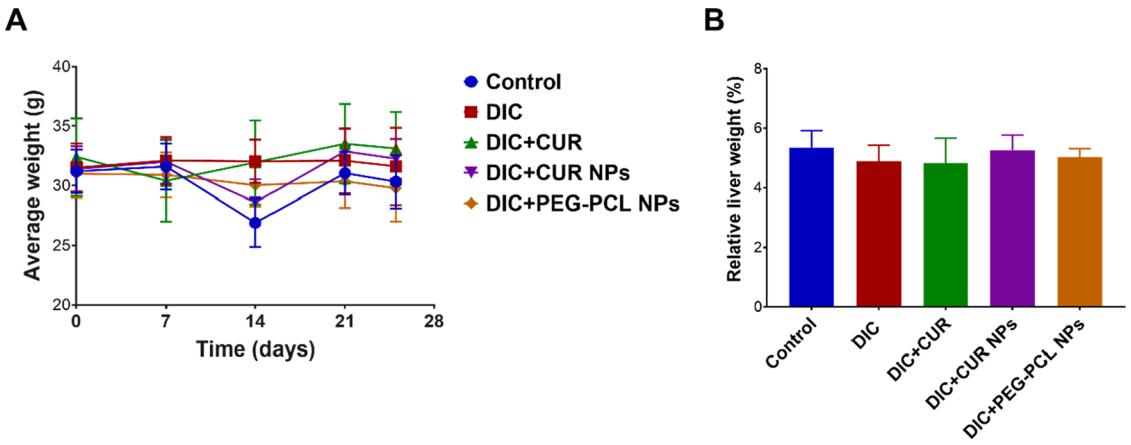

Figure 2. Physical observation of the experimental mice throughout the study. No significant changes in mice weights (A) or liver weights relative to the total weight (B) were observed among the negative control and treated groups.

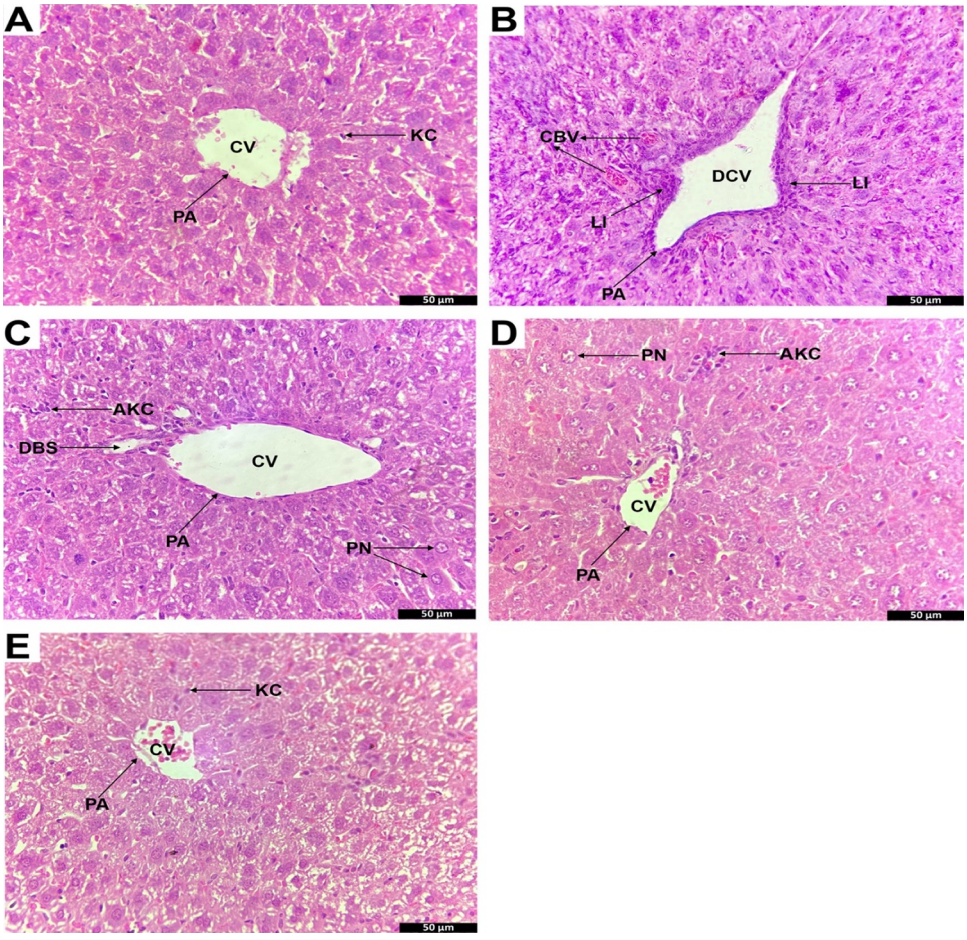

Figure 3. Histopathological examination of the liver sections of the (A) negative control (vehicle), (B) DIC (positive control), (C) DIC+CUR, (D) DIC+PEG−PCL NPs, and (E) DIC+CUR NPs groups.

Approximately, 4.8% of the loaded drug was released within 24 h, and 31.9% was released after 96 h. Free CUR showed faster release kinetics in the first 8 h compared to the NPs, achieving almost complete release after 96 h and ruling out any artifacts arising from the dialysis membrane. Based on these results, CUR NPs could be employed as a CUR drug delivery system because of their sustained release property.

Effect of CUR and CUR NPs on DIC-Induced Liver Injury in Mice. Figure 2A represents the change in body weight of all animal groups on the first, seventh, 14th, 21st, and 25th day of the study, where in the first 2 days, the DIC+CUR and DIC+CUR NPs groups received daily IP injections of each treatment, followed by 23 days of treatment with DIC. There was no significant difference ($p > 0.05$) in the mices' body weights throughout the period of the study according to two-way ANOVA. Likewise, there was no significant difference ($p > 0.05$) in the liver weights relative to the total animal body

https://doi.org/10.1021/acsomega.3c07602
ACS Omega 2024, 9, 7881−7890

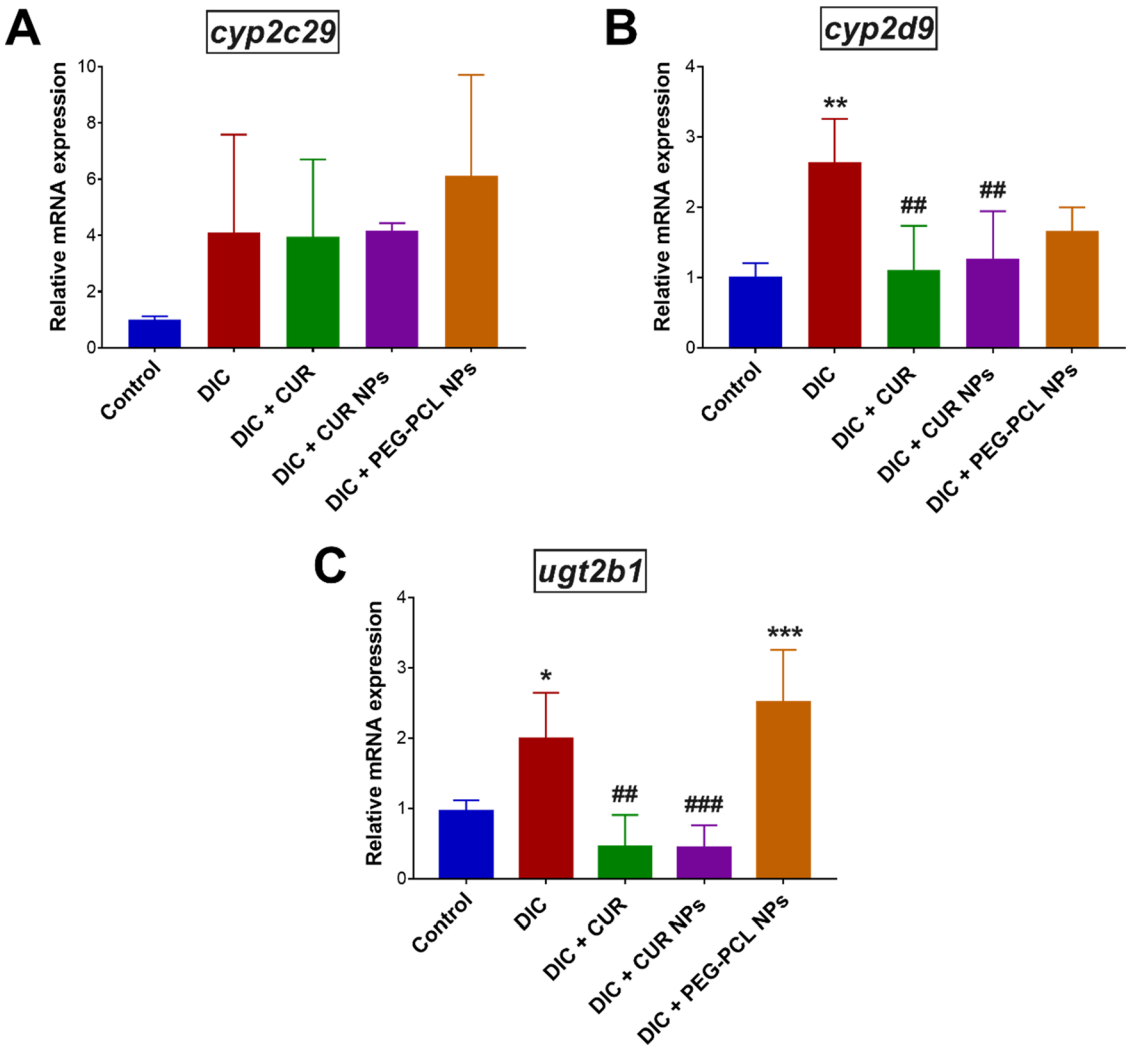

Figure 4. Relative mRNA expression of (A) *cyp2c29*, (B) *cyp2d9*, and (C) *ugt2b1* in the livers of mice treated with DIC (positive control), DIC +CUR, DIC+CUR NPs, and DIC+PEG−PCL NPs compared with the negative control (vehicle-treated group). Results represent the mean ± SD (n = 5). *p < 0.05, **p < 0.01, and ***p < 0.001 compared to the negative control. $^{\#\#}p$ < 0.01 and $^{\#\#\#}p$ < 0.001 compared to the DIC group (positive control) based on one-way ANOVA followed by Tukey's post-hoc test.

weight between the control group and all the other treated groups at the end of the study (Figure 2B).

Histological Analysis. Figure 3 represents histological sections of mice livers after different treatment conditions. The negative control group (Figure 3A) revealed a normal histological appearance of Kupffer cells (KC), central vein (CV), and the portal area (PA). On the other hand, the DIC group (positive control; Figure 3B) was associated with the appearance of dilated central vein (DCV), inflammatory cells and leukocyte infiltrations (LI), and congested blood vessels (CBV) in the PA. The liver sections of the DIC+CUR group (Figure 3C) also exhibited signs of liver injury that manifested as activated Kupffer cells (AKC), pyknotic nuclei (PN), and dilatation in blood sinusoids (DBS), CV, and PA. The DIC +PEG−PCL NPs group (Figure 3D) exhibited a DCV, LI, and CBV in the PA. Conversely, in the DIC+CUR NPs group (Figure 3E), the liver sections were approximating the control group, with the appearance of KC, CV, and PA.

mRNA Levels of Drug-Metabolizing Cyp450s and Ugt Genes. Treatment with DIC, DIC+CUR, DIC+CUR NPs, and DIC+PEG−PCL NPs exhibited varying effects on the expression of drug-metabolizing *Cyp450* and *Ugt* genes in the livers of the treated mice. As shown in Figure 4A, no significant difference was found in the relative mRNA expression of *cyp2c29* of the various treatment groups compared to the negative control (p > 0.05). In the case of *cyp2d9* (Figure 4B), DIC treatment (positive control) resulted in a 2.6-fold increase in the relative gene expression compared with the negative control (p < 0.01), while the DIC + CUR and DIC + CUR NPs groups were found to be similar to the negative control (p > 0.05). The two groups were also associated with significantly lower *cyp2d9* mRNA expression levels compared with the DIC group (p < 0.01). In the DIC + PEG−PCL NPs group, no significant difference was found in the gene expression of *cyp2d9* compared with the negative control and the DIC group (p > 0.05). As for *ugt2b1* (Figure 4C), DIC treatment resulted in a 2.2-fold increase in gene expression compared with the negative control (p < 0.01), while both DIC + CUR and DIC + CUR NPs maintained normal expression levels which were significantly lower than the DIC group (p < 0.0001). DIC + PEG−PCL NPs caused a 2.8-fold increase in gene expression compared with the negative control group (p < 0.0001) which was not significantly different than the DIC group (p > 0.05).

https://doi.org/10.1021/acsomega.3c07602
ACS Omega 2024, 9, 7881−7890

DISCUSSION

CUR is a polyphenol derived from *Curcuma longa L*. It has a beneficial effect as neuroprotective, hepatoprotective, wound healing, and antidiabetic agent.[41] Because of CUR's hepatoprotective benefits, it was hypothesized in this study that it could protect the liver against DIC-induced toxicity. CUR was applied in a free form as well as a polymeric NP formulation, which was developed to circumvent its delivery challenges and biopharmaceutical limitations. Several nanoscale formulation strategies have been attempted to improve the delivery efficacy of CUR and maximize its therapeutic benefits, including liposomes, solid lipid NPs, micelles, gold NPs, nanoemulsions, and polymeric NPs.[42] In this study, CUR was loaded in the biocompatible amphiphilic copolymer PEG−PCL by employing the nanoprecipitation method. This method was first described by Fessi et al. and represents a robust encapsulation technique for hydrophobic drugs.[34] The physicochemical properties of the formed NPs such as size, polydispersity, and drug loading efficiency are influenced by several factors, including the ratio of the organic/aqueous phase, the polymer concentration, the polymer MW, and the drug concentration.[43] Herein, the drug concentration was varied while the ratio of the organic/aqueous phase, the polymer concentration, and the polymer MW remained constant. An excellent CUR loading efficiency was obtained (82.4−93.1%) which was better than the loading efficiency range of 13.4−55.7% of a previous study, where the self-assembly properties of tannic acid were employed to produce CUR-loaded NPs.[44]

The particle size obtained for CUR NPs was between 64.0 and 67.4 nm, with high monodispersity as indicated by the low PDI values (0.08−0.09). The particle size was robust and was below 100 nm. Previous studies have shown that NP size can affect their biodistribution, with sizes below 200 nm being preferred for longer circulation times.[45] In particular, PEG−PCL NPs with PEG MW of 5000 and sizes around 100 nm resisted opsonization and exhibited prolonged circulation times.[46] In vitro drug release revealed sustained release kinetics compared with the free drug, with a delay in drug release in the first 8 h followed by a sustained release for 96 h. This pattern of sustained release is likely attributed to the time required to degrade the PEG−PCL.[33]

Next, we investigated the potential hepatoprotective role of CUR NPs in an animal model of DIC-induced liver injury. In the in vivo experiments, although no physical changes were observed in terms of the weight of mice and their livers at the end of the study, histopathological changes were evident. Notable abnormalities were observed in the livers of the DIC group compared with the control, including a DCV, LI, and CBV in the PA. These results are in agreement with a previous study that showed histopathological alterations of the liver sections of mice administered DIC at 4 and 14 mg/kg daily, where the liver tissue damage was evident after 14, 21, and 28 days for both doses.[36] Upon administration of free CUR, the DIC+CUR group maintained some histopathological signs of liver injury. Al-Dossari et al. reported that concomitant administration of CUR (200 mg/kg) and selenium (0.1 mg/kg) for 7 days protected the livers of experimental rats against acute liver injury resulting from a single dose of DIC (20 mg/kg) along with LPS (10 μg/kg).[47] Another study demonstrated that 200 mg/kg CUR for 7 days protected rats' livers against DIC-induced hepatotoxicity, where DIC was administered as a single dose of 150 mg/kg.[48] Since CUR (log P of ∼3) is classified as a Class IV drug according to the Biopharmaceutics Classification System (BCS), it is evident that the bioactivity of CUR could be hindered by its poor bioavailability, necessitating the administration of doses as high as 200 mg/kg.[49] In this study, CUR was administered at a lower dose of 20 mg/kg. While the DIC+CUR group did not exhibit a complete reversal of liver injury, liver sections of the DIC +CUR NPs group showed almost normal histological appearance with an absence of inflammatory signs such as DCV, CBV, or LI. This strongly indicates that nanoencapsulation of CUR can enhance its hepatoprotective activity, which may be attributed to a combination of factors including enhanced solubility, permeability, and sustained release. Our findings are supported by a previous study in rats which showed that CUR loaded in PCL−PEG−PCL triblock copolymer NPs exhibited a prolonged half-life and enhanced liver accumulation compared to free CUR, where the latter was rapidly eliminated in the bile after intravenous administration.[50] Conversely, the livers of the DIC+PEG−PCL NPs group resembled the DIC group in appearance, reflecting the inert nature of the empty NPs.

Previous studies have reported on the development of CUR nanocarriers to improve its efficacy as a hepatoprotective agent. For example, green-synthesized silver NPs coated with CUR and chitosan were found to be effective against CCl_4-induced liver fibrosis in a mouse model.[51] CUR encapsulated in poly(lactide-*co*-glycolide) (PLGA) NPs showed greater cytotoxicity against HepG2 liver cancer cells in vitro and enhanced liver accumulation in vivo compared to free CUR.[52] Another study found that CUR loaded in PEG-polylactide (PEG−PLA) NPs mitigated the histopathological and inflammatory changes in the livers of diabetic rats.[53] Similarly, CUR in the form of nanomicelles exhibited pronounced hepatoprotective activity against paraquat-induced liver injury compared to free CUR,[54] while CUR loaded in solid lipid NPs efficiently protected rat livers against acetaminophen-induced hepatotoxicity.[55] Although CUR has previously been formulated in PEG−PCL micelles/NPs, the formulations were only evaluated in vitro in terms of their physicochemical properties[56] and in vivo for anticancer therapy.[57] To the best of our knowledge, this is the first investigation of the potential hepatoprotective effect of PEG−PCL-based CUR NPs. Our findings signify that CUR NPs were able to exert a protective effect on the liver, most likely due to CUR's anti-inflammatory and antioxidant properties, consistent with previous reports.

We looked at the potential involvement of CYP450 enzymes in DIC-induced liver injury and whether it could be mitigated by CUR and/or its NP formulation. Gene expression analysis of *cyp2c29* revealed no significant change in its expression across the different treatment groups, which is in agreement with our previous study where DIC was administered at 10 mg/kg to mice for 14 days.[17] Note that DIC is metabolized by CYP2C9 in humans (equivalent to cyp2c29 in mice), producing oxidized metabolites that contribute to its hepatotoxicity. On the other hand, both *cyp2d9* and *ugt2b1* genes were significantly upregulated by DIC treatment. Our previous study showed that DIC treatment at 10 mg/kg for 14 days significantly downregulated the expression of *ugt2b1*,[18] implying that DIC's role in modulating the expression of CYP450 enzymes is time-dependent. *Ugt2b1* in mice is analogous to UGT2B7 in humans, which is involved in DIC's conjugation. Similar to CYP2C9, UGT2B7 has also

https://doi.org/10.1021/acsomega.3c07602
ACS Omega 2024, 9, 7881−7890

been linked to DIC-induced hepatotoxicity.[58] No previous study has linked DIC to cyp2d9 or its corresponding human enzyme, CYP2D6, where the latter is not thought to be induced by classic mechanisms of enzyme induction.[59] Nonetheless, the upregulation in *cyp2d9* and *ugt2b1* expression resulting from DIC administration was normalized upon the administration of both CUR and CUR NPs, which strongly indicates that CUR can mitigate hepatic enzymes' dysregulation caused by DIC. Note that free CUR was as effective as CUR NPs in modulating gene expression of the drug-metabolizing enzymes, which suggests that low doses of CUR may be sufficient to achieve this effect.

CONCLUSIONS

The encapsulation of CUR in PEG−PCL NPs provides an attractive delivery strategy to improve its poor water solubility and/or permeability for in vivo applications. CUR NPs exhibited excellent physicochemical characteristics and enhanced hepatoprotective effects in DIC-induced liver injury, most likely due to improved liver uptake of nanoencapsulated CUR. An investigation of the hepatic drug-metabolizing enzymes cyp2d9 and ugt2b1 (corresponding to human CYP2D6 and UGT2B7, respectively) revealed a putative link between DIC-induced liver injury and altered gene expression of these drug-metabolizing enzymes. This effect was normalized upon the administration of both free CUR and CUR NPs, despite the low bioavailability of free CUR, which implies that a low dose of CUR could be sufficient to exert this effect. Taken together, our findings provide insights into the promising role of CUR NPs as a nutraceutical formulation that can overcome the biopharmaceutical limitations of free CUR and mitigate the hepatic side effects associated with chronic NSAIDs use.

AUTHOR INFORMATION

Corresponding Author

Suhair Sunoqrot − *Department of Pharmacy, Faculty of Pharmacy, Al-Zaytoonah University of Jordan, Amman 11733, Jordan;* orcid.org/0000-0001-8810-1751; Email: suhair.sunoqrot@zuj.edu.jo

Authors

Mohammad Abu Shalhoob − *Department of Pharmacy, Faculty of Pharmacy, Al-Zaytoonah University of Jordan, Amman 11733, Jordan*

Yazun Jarrar − *Department of Basic Medical Sciences, Faculty of Medicine, Al-Balqa Applied University, Al-Salt 19117, Jordan*

Alaa M. Hammad − *Department of Pharmacy, Faculty of Pharmacy, Al-Zaytoonah University of Jordan, Amman 11733, Jordan*

Hamzeh J. Al-Ameer − *Department of Pharmaceutical Biotechnology, Faculty of Allied Medical Sciences, Al-Ahliyya Amman University, Amman 19328, Jordan;* orcid.org/0000-0002-1681-6747

Wajdy Al-Awaida − *Department of Biology and Biotechnology, American University of Madaba, Madaba 17110, Jordan*

Complete contact information is available at: https://pubs.acs.org/10.1021/acsomega.3c07602

Notes

The authors declare no competing financial interest.

ACKNOWLEDGMENTS

This work was supported by Al-Zaytoonah University of Jordan (grant no. 14/08/2021-2022). The authors thank Ms Lujain Alzaghari for assistance with RT-PCR analysis.

REFERENCES

(1) Almazroo, O. A.; Miah, M. K.; Venkataramanan, R. Drug Metabolism in the Liver. *Clin. Liver. Dis.* **2017**, *21* (1), 1−20.

(2) Woolbright, B. L.; Jaeschke, H. Mechanisms of inflammatory liver injury and drug-induced hepatotoxicity. *Curr. Pharmacol. Rep.* **2018**, *4* (5), 346−357.

(3) Iyanagi, T. Molecular mechanism of phase I and phase II drug-metabolizing enzymes: implications for detoxification. *Int. Rev. Cytol.* **2007**, *260*, 35−112.

(4) Amacher, D. E. The primary role of hepatic metabolism in idiosyncratic drug-induced liver injury. *Expert. Opin. Drug Metab. Toxicol.* **2012**, *8* (3), 335−347.

(5) García-cortés, M.; Ortega-alonso, A.; Lucena, M. I.; Andrade, R. J. Drug-induced liver injury: a safety review. *Expert Opin. Drug Saf.* **2018**, *17* (8), 795−804.

(6) Zhou, S.; Chan, E.; Duan, W.; Huang, M.; Chen, Y.-Z. Drug bioactivation covalent binding to target proteins and toxicity relevance. *Drug Metab. Rev.* **2005**, *37* (1), 41−213.

(7) Villeneuve, J. P.; Pichette, V. Cytochrome P450 and liver diseases. *Curr. Drug Metab.* **2004**, *5* (3), 273−282.

(8) Harirforoosh, S.; Jamali, F. Renal adverse effects of nonsteroidal anti-inflammatory drugs. *Expert Opin. Drug Saf.* **2009**, *8* (6), 669−681.

(9) Knights, K. M.; Winner, L. K.; Elliot, D. J.; Bowalgaha, K.; Miners, J. O. Aldosterone glucuronidation by human liver and kidney microsomes and recombinant UDP-glucuronosyltransferases: Inhibition by NSAIDs. *Br. J. Clin. Pharmacol.* **2009**, *68* (3), 402−412.

(10) Essex, M. N.; Zhang, R. Y.; Berger, M. F.; Upadhyay, S.; Park, P. W. Safety of celecoxib compared with placebo and non-selective NSAIDs: cumulative meta-analysis of 89 randomized controlled trials. *Expert Opin. Drug. Saf.* **2013**, *12* (4), 465−477.

(11) Bennett, W. M.; Henrich, W. L.; Stoff, J. S. The renal effects of nonsteroidal anti-inflammatory drugs: summary and recommendations. *Am. J. Kidney Dis.* **1996**, *28* (1), S56−S62.

(12) Mcgettigan, P.; Henry, D. Use of non-steroidal anti-inflammatory drugs that elevate cardiovascular risk: an examination of sales and essential medicines lists in low-, middle-, and high-income countries. *PLoS Med.* **2013**, *10* (2), No. e1001388.

(13) Altman, R.; Bosch, B.; Brune, K.; Patrignani, P.; Young, C. Advances in NSAID development: evolution of diclofenac products using pharmaceutical technology. *Drugs* **2015**, *75* (8), 859−877.

(14) Jiang, W.; Dai, T.; Xie, S.; Ding, L.; Huang, L.; Dai, R. Roles of diclofenac and its metabolites in immune activation associated with acute hepatotoxicity in TgCYP3A4/hPXR-humanized mice. *Int. Immunopharmacol.* **2020**, *86*, No. 106723.

(15) Tang, W. The metabolism of diclofenac-enzymology and toxicology perspectives. *Curr. Drug Metab.* **2003**, *4* (4), 319−329.

(16) Gómez-lechón, M. J.; Ponsoda, X.; O'connor, E.; Donato, T.; Castell, J. V.; Jover, R. Diclofenac induces apoptosis in hepatocytes by alteration of mitochondrial function and generation of ROS. *Biochem. Pharmacol.* **2003**, *66* (11), 2155−2167.

(17) Jarrar, Y.; Jarrar, Q.; Abu-shalhoob, M. Effects of nonsteroidal anti-inflammatory drugs on the expression of arachidonic acid-metabolizing Cyp450 genes in mouse hearts, kidneys and livers. *Prostaglandins Other Lipid Mediators* **2019**, *141*, 14−21.

(18) Jarrar, Y.; Jarrar, Q.; Abu-shalhoob, M.; Sha'ban, E. Relative expression of mouse udp-glucuronosyl transferase 2b1 gene in the livers, kidneys, and hearts: The influence of nonsteroidal anti-inflammatory drug treatment. *Curr. Drug Metab.* **2019**, *20* (11), 918−923.

(19) Singh, D.; Cho, W. C.; Upadhyay, G. Drug-induced liver toxicity and prevention by herbal antioxidants: An overview. *Front. Physiol.* **2016**, *6*, 363.

(20) Zaidi, S. M. K. R.; Al-Qirim, T. M.; Banu, N. Effects of antioxidant vitamins on glutathione depletion and lipid peroxidation induced by restraint stress in the rat liver. *Drugs R&D* **2005**, *6* (3), 157−165.
(21) Deogade, S. C.; Ghate, S. Curcumin: therapeutic applications in systemic and oral health. *Int. J. Biol. Pharm. Res.* **2015**, *6* (4), 281−290.
(22) Prasad, S.; Gupta, S. C.; Tyagi, A. K.; Aggarwal, B. B. Curcumin, a component of golden spice: from bedside to bench and back. *Biotechnol. Adv.* **2014**, *32* (6), 1053−1064.
(23) Shehzad, A.; Rehman, G.; Lee, Y. S. Curcumin in inflammatory diseases. *Biofactors* **2013**, *39* (1), 69−77.
(24) Vera-ramirez, L.; Pérez-lopez, P.; Varela-lopez, A.; Ramirez-tortosa, M.; Battino, M.; Quiles, J. L. Curcumin and liver disease. *Biofactors* **2013**, *39* (1), 88−100.
(25) Panahi, Y.; Valizadegan, G.; Ahamdi, N.; Ganjali, S.; Majeed, M.; Sahebkar, A. Curcuminoids plus piperine improve nonalcoholic fatty liver disease: A clinical trial. *J. Cell. Biochem.* **2019**, *120* (9), 15989−15996.
(26) Krishnareddy, N. T.; Thomas, J. V.; Nair, S. S.; M, J. N.; Maliakel, B. P.; Krishnakumar, I. M. A Novel Curcumin-Galactomannoside Complex Delivery System Improves Hepatic Function Markers in Chronic Alcoholics: A Double-Blinded, randomized, Placebo-Controlled Study. *Biomed. Res. Int.* **2018**, *2018*, No. 9159281.
(27) Quispe, C.; Cruz-martins, N.; Manca, M. L.; Manconi, M.; Sytar, O.; Hudz, N.; Shanaida, M.; Kumar, M.; Taheri, Y.; Martorell, M. Nano-derived therapeutic formulations with curcumin in inflammation-related diseases. *Oxid. Med. Cell. Longev.* **2021**, *2021*, No. 3149223.
(28) Salehi, B.; Del prado-audelo, M. L.; Cortés, H.; Leyva-gómez, G.; Stojanović-radić, Z.; Singh, Y. D.; Patra, J. K.; Das, G.; Martins, N.; Martorell, M. Therapeutic applications of curcumin nanomedicine formulations in cardiovascular diseases. *J. Clin. Med.* **2020**, *9* (3), 746.
(29) Sohn, S.-I.; Priya, A.; Balasubramaniam, B.; Muthuramalingam, P.; Sivasankar, C.; Selvaraj, A.; Valliammai, A.; Jothi, R.; Pandian, S. Biomedical applications and bioavailability of curcumin—An updated overview. *Pharmaceutics* **2021**, *13* (12), 2102.
(30) Garbayo, E.; Pascual-gil, S.; Rodríguez-nogales, C.; Saludas, L.; Estella-hermoso de mendoza, A.; Blanco-prieto, M. J. Nanomedicine and drug delivery systems in cancer and regenerative medicine. *Wiley Interdiscip. Rev. Nanomed. Nanobiotechnol.* **2020**, *12* (5), No. e1637.
(31) Patra, J. K.; Das, G.; Fraceto, L. F.; Campos, E. V. R.; Rodriguez-torres, M. D. P.; Acosta-torres, L. S.; Diaz-torres, L. A.; Grillo, R.; Swamy, M. K.; Sharma, S.; Habtemariam, S.; Shin, H. S. Nano based drug delivery systems: recent developments and future prospects. *J. Nanobiotechnology* **2018**, *16* (1), 71.
(32) Begines, B.; Ortiz, T.; Pérez-aranda, M.; Martínez, G.; Merinero, M.; Argüelles-arias, F.; Alcudia, A. Polymeric nanoparticles for drug delivery: recent developments and future prospects. *Nanomaterials* **2020**, *10* (7), 1403.
(33) Sunoqrot, S.; Alsadi, A.; Tarawneh, O.; Hamed, R. Polymer type and molecular weight dictate the encapsulation efficiency and release of Quercetin from polymeric micelles. *Colloid Polym. Sci.* **2017**, *295* (10), 2051−2059.
(34) Fessi, H.; Puisieux, F.; Devissaguet, J. P.; Ammoury, N.; Benita, S. Nanocapsule formation by interfacial polymer deposition following solvent displacement. *Int. J. Pharm.* **1989**, *55* (1), R1−R4.
(35) Olfert, E. D.; Cross, B. M.; Mcwilliam, A. A. *Guide to the care and use of experimental animals*; Canadian Council on Animal Care: Ottawa, 1993; Vol. *1*.
(36) Mohan, D.; Sharma, S. Histopathological alterations in liver of mice exposed to different doses of diclofenac sodium. *Int. J. Anim. Vet. Sci.* **2017**, *11* (11), 738−742.
(37) Al-shalabi, E.; Abusulieh, S.; Hammad, A. M.; Sunoqrot, S. Rhoifolin loaded in PLGA nanoparticles alleviates oxidative stress and inflammation in vitro and in vivo. *Biomater. Sci.* **2022**, *10* (19), 5504−5519.
(38) Livak, K. J.; Schmittgen, T. D. Analysis of relative gene expression data using real-time quantitative PCR and the $2^{-\Delta\Delta CT}$ method. *Methods* **2001**, *25* (4), 402−408.
(39) Tawfik, V. L.; Lacroix-fralish, M. L.; Bercury, K. K.; Nutile-mcmenemy, N.; Harris, B. T.; Deleo, J. A. Induction of astrocyte differentiation by propentofylline increases glutamate transporter expression in vitro: heterogeneity of the quiescent phenotype. *Glia* **2006**, *54* (3), 193−203.
(40) Al-shalabi, E.; Alkhaldi, M.; Sunoqrot, S. Development and evaluation of polymeric nanocapsules for cirsiliol isolated from Jordanian *Teucrium polium* L. as a potential anticancer nanomedicine. *J. Drug Delivery Sci. Technol.* **2020**, *56*, No. 101544.
(41) Ma, Z.; Wang, N.; He, H.; Tang, X. Pharmaceutical strategies of improving oral systemic bioavailability of curcumin for clinical application. *J. Controlled Release* **2019**, *316*, 359−380.
(42) Karthikeyan, A.; Senthil, N.; Min, T. Nanocurcumin: A promising candidate for therapeutic applications. *Front. Pharmacol.* **2020**, *11*, 487.
(43) Martínez rivas, C. J.; Tarhini, M.; Badri, W.; Miladi, K.; Greige-gerges, H.; Nazari, Q. A.; Galindo rodríguez, S. A.; Román, R. Á.; Fessi, H.; Elaissari, A. Nanoprecipitation process: From encapsulation to drug delivery. *Int. J. Pharm.* **2017**, *532* (1), 66−81.
(44) Sunoqrot, S.; Orainee, B.; Alqudah, D. A.; Daoud, F.; Alshaer, W. Curcumin-tannic acid-poloxamer nanoassemblies enhance curcumin's uptake and bioactivity against cancer cells in vitro. *Int. J. Pharm.* **2021**, *610*, No. 121255.
(45) Kulkarni, S. A.; Feng, S.-S. Effects of particle size and surface modification on cellular uptake and biodistribution of polymeric nanoparticles for drug delivery. *Pharm. Res.* **2013**, *30* (10), 2512−2522.
(46) Wang, J.-L.; Du, X.-J.; Yang, J.-X.; Shen, S.; Li, H.-J.; Luo, Y.-L.; Iqbal, S.; Xu, C.-F.; Ye, X.-D.; Cao, J.; Wang, J. The effect of surface poly(ethylene glycol) length on in vivo drug delivery behaviors of polymeric nanoparticles. *Biomaterials* **2018**, *182*, 104−113.
(47) Al-dossari, M. H.; Fadda, L. M.; Attia, H. A.; Hasan, I. H.; Mahmoud, A. M. Curcumin and selenium prevent lipopolysaccharide/diclofenac-induced liver injury by suppressing inflammation and oxidative stress. *Biol. Trace Elem. Res.* **2020**, *196*, 173−183.
(48) Ali, E. M. Protective effect of curcumin on diclofenac sodium-induced hepatotoxicity in male albino rats: Evidence of its antioxidant and anti-inflammatory properties. *Record. Pharm. Biomed. Sci.* **2022**, *6* (3), 195−206.
(49) Ipar, V. S.; Dsouza, A.; Devarajan, P. V. Enhancing curcumin oral bioavailability through nanoformulations. *Eur. J. Drug Metab. Pharmacokinet.* **2019**, *44* (4), 459−480.
(50) Guo, F.; Guo, D.; Zhang, W.; Yan, Q.; Yang, Y.; Hong, W.; Yang, G. Preparation of curcumin-loaded PCL-PEG-PCL triblock copolymeric nanoparticles by a microchannel technology. *Eur. J. Pharm. Sci.* **2017**, *99*, 328−336.
(51) Elzoheiry, A.; Ayad, E.; Omar, N.; Elbakry, K.; Hyder, A. Anti-liver fibrosis activity of curcumin/chitosan-coated green silver nanoparticles. *Sci. Rep.* **2022**, *12* (1), 18403.
(52) Chen, X.-P.; Li, Y.; Zhang, Y.; Li, G.-W Formulation, characterization and evaluation of curcumin-loaded PLGA-TPGS nanoparticles for liver cancer treatment. *Drug Des., Dev. Ther.* **2019**, *13*, 3569−3578.
(53) El-naggar, M. E.; Al-joufi, F.; Anwar, M.; Attia, M. F.; El-bana, M. A. Curcumin-loaded PLA-PEG copolymer nanoparticles for treatment of liver inflammation in streptozotocin-induced diabetic rats. *Colloids Surf., B* **2019**, *177*, 389−398.
(54) Kheiripour, N.; Plarak, A.; Heshmati, A.; Asl, S. S.; Mehri, F.; Ebadollahi-natanzi, A.; Ranjbar, A.; Hosseini, A. Evaluation of the hepatoprotective effects of curcumin and nanocurcumin against paraquat-induced liver injury in rats: Modulation of oxidative stress and Nrf2 pathway. *J. Biochem. Mol. Toxicol.* **2021**, *35* (5), No. e22739.
(55) Hussein, R. M.; Kandeil, M. A.; Mohammed, N. A.; Khallaf, R. A. Evaluation of the hepatoprotective effect of curcumin-loaded solid lipid nanoparticles against paracetamol overdose toxicity: Role of

https://doi.org/10.1021/acsomega.3c07602
ACS Omega 2024, 9, 7881−7890

inducible nitric oxide synthase. *J. Liposome Res.* **2022**, *32* (4), 365−375.
(56) Danafar, H.; Davaran, S.; Rostamizadeh, K.; Valizadeh, H.; Hamidi, M. Biodegradable m-PEG/PCL core-shell micelles: preparation and characterization as a sustained release formulation for curcumin. *Adv. Pharm. Bull.* **2014**, *4* (Suppl 2), 501−510.
(57) Manjili, H. K.; Sharafi, A.; Danafar, H.; Hosseini, M.; Ramazani, A.; Ghasemi, M. H. Poly(caprolactone)−poly(ethylene glycol)−poly(caprolactone) (PCL−PEG−PCL) nanoparticles: a valuable and efficient system for in vitro and in vivo delivery of curcumin. *RSC Adv.* **2016**, *6* (17), 14403−14415.
(58) Tolosa, L.; Jiménez, N.; Pérez, G.; Castell, J. V.; Gómez-lechón, M. J.; Donato, M. T. Customised in vitro model to detect human metabolism-dependent idiosyncratic drug-induced liver injury. *Arch. Toxikol.* **2018**, *92* (1), 383−399.
(59) Amaeze, O. U.; Czuba, L. C.; Yadav, A. S.; Fay, E. E.; Lafrance, J.; Shum, S.; Moreni, S. L.; Mao, J.; Huang, W.; Isoherranen, N.; Hebert, M. F. Impact of pregnancy and vitamin A supplementation on CYP2D6 activity. *J. Clin. Pharmacol.* **2023**, *63* (3), 363−372.

NOTE ADDED AFTER ASAP PUBLICATION

This paper originally published ASAP on January 31, 2024. Reference 20 was changed, and a new version of the paper reposted on February 5, 2024.

https://doi.org/10.1021/acsomega.3c07602
ACS Omega 2024, 9, 7881−7890